

## Electromagnetic Lensing Using a Ferrofluid Thin Film

Timm A Vanderelli

Primary Investigator, Ferrocell USA, Ligonier, Pennsylvania, 15658 USA

## \*Corresponding author

Timm A Vanderelli, Primary Investigator, Ferrocell USA, Ligonier, Pennsylvania, 15658 USA.

Received: March 11, 2024; Accepted: March 25, 2024; Published: March 30, 2024

## ABSTRACT

In this report, I show by experiment how a Ferrofluid thin-film contained between two flat glass disks, referred to here as a “Ferrocell”, will create a circular disk pattern on a target using laser and a parallel, homogeneous electromagnetic field from a Helmholtz coil with a strong correlation to the circular disk pattern produced by a glass Plano- concave lens. Furthermore, I show how this circular pattern will increase or decrease in diameter, depending on the location of the Ferrocell between a laser source and a target while induced within an electromagnetic field.

## Introduction

A Ferrocell or Ferrolens is comprised of two flat disks of optical glass separated by a thin-film of Ferrotec EFH1 Ferrofluid with a saturation magnetization of 400 Gauss, a viscosity of 6 cp @ 27 C and a particle density of 1.21 gm/ml [1,2]. This thin-film is sealed between the glass disks with a bead of Norland No. 81 UV cured, optical adhesive around its circumference. In recently published papers written about the optical response of Ferrocells, other researchers have shown how this device will scatter light in a direction determined by the orientation of a magnetic field using externally applied permanent magnets and LED light sources [3-7]. Here, I report how the cell responds when induced within the center of a parallel electromagnetic field from an air-core Helmholtz coil. Consisting of two 140 mm outside diameter, 90 mm inside diameter, 45 mm wide spools, each using 68 meters of 12 gauge, square, enameled, copper wire and spaced apart 70 mm (center to center), with a combined (series connected) DC resistance of 400 milli- Ohms and a combined inductance of 4 mH. For the following tests, two clear, 62mm diameter x 2 mm thick borosilicate flat glass disks were used, with a 30 $\mu$ m layer of Ferrofluid equally dispersed and sealed between them. In this thin-film condition, the fluid layer is translucent instead of its normally opaque condition. During the following tests, the Ferrocell was operated in the transmission mode and irradiated by a one-Watt, 532 nm laser using a regulated, variable output, power supply. Without an applied field, the thin-film’s suspended and coated magnetite nanoparticles exist in a Superparamagnetic state, functioning in a similar manner to a nonlinear, bandpass optical filter, exhibiting a high degree of absorption in the shorter wavelengths, as shown by spectrometer measurement in the following two Figures [8]. A white Halogen light source

was used as a reference without the cell installed as indicated by an absorption spectrograph of relative linear amplitude units on the Y-axis and between 450 and 700 nm wavelengths across the X-axis, as shown in Figure 1.

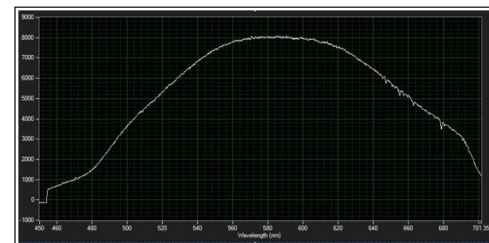


Figure 1: Absorption spectrum of Halogen light for reference.

White Halogen light transmitted through and absorbed by a Ferrocell centrally located between both un-activated inductors of the Helmholtz coil is shown in spectrograph, Figure 2. The shorter wavelengths are highly attenuated while the longer wavelengths pass easily to 600 nm, then begin to attenuate again. The cell responds like a bandpass filter, centered at 640 nm

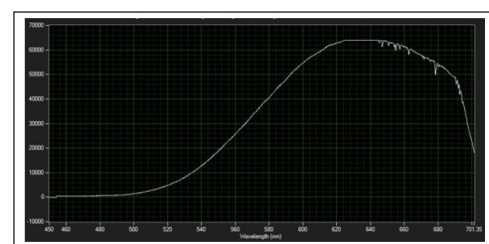
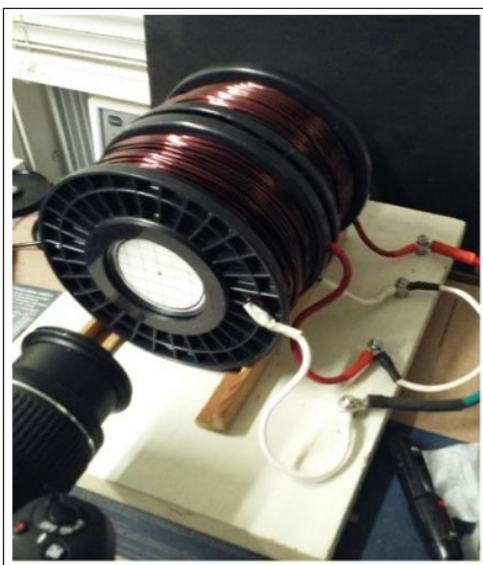


Figure 2: Absorption spectrograph Halogen light transmitted through the 30 micron thin-film

However, with the application of an electromagnetic field, the nanoparticles coalesce into microscopic ( $\sim 100 \mu\text{m}$ ) chains that change the particles response into a ferrimagnetic state [9,10]. While in this state, these dynamic particle chains scatter light in a direction and a manner determined by the parallel polar orientation of the induced field [11]. The following tests and examples show how a Ferrocell, when located inside an air-core Helmholtz coil, will scatter laser into a circular beam pattern on a target, which is then compared to a circular beam pattern obtained from a Plano-concave (PCV) glass lens, as shown by test results obtained through experiment and measurement.

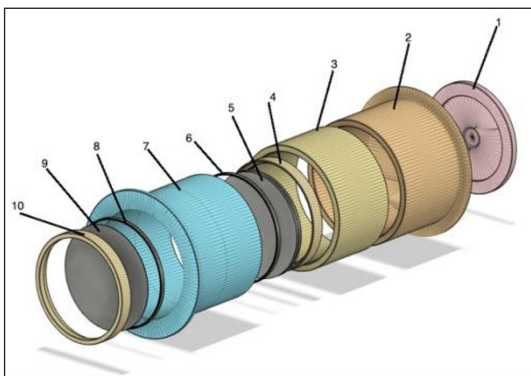
## Experiments

A cylindrical insert was fabricated using black ABS plastic through a 3-D printer and inserted into the center of the Helmholtz inductors. A photo of this insert is shown in Figure 3 while Figure 4 shows a CAD drawing of it as an exploded view with a legend for reference.



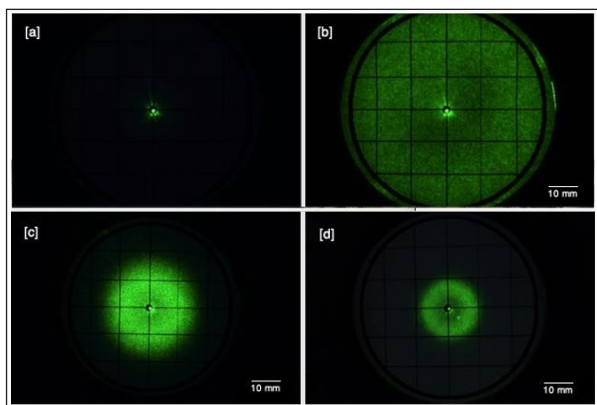
**Figure 3:** Helmholtz coil. Insert, target, camera and connections visible.

This test apparatus includes a laser source mounted into an insert located in the rear, south pole of the unit. An ABS plastic diaphragm with a one-millimeter diameter aperture was positioned 5 mm from the laser output. A first target consisting of a 55 mm disk of typical bright-white printer paper with a 2 mm black dot in the center and a thin grid of 10 mm squares was fixed into the opposing north pole insert at the front of this unit for taking photos without saturating the camera's CCD sensor by laser.

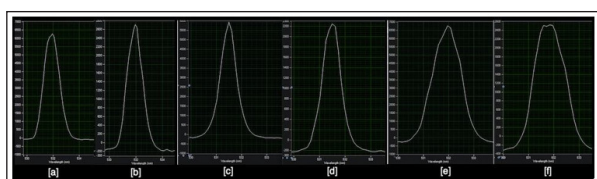


**Figure 4:** Helmholtz coil insert exploded view with numbered parts.

Referring to Figure 4, numbered parts are [1] aperture, [2] rear insert, [3] tunnel, [4] lock ring A, [5] Ferrocell, [6] lock ring B, [7] front insert, [8] lock ring C, [9] target and [10] lock ring D. A second target was constructed without a center dot or grid-lines using the same bright-white paper to prevent saturation of the beam profiler camera's CCD sensor. The Ferrocell or the Plano-concave lens can be positioned at any specific location between electromagnetic poles within this light-proof tunnel, including any location inside of both front and rear inserts. In the following three experiments, a Ferrocell was moved closer to or farther away from the target while inside the electromagnetic field while irradiated with laser. This action altered the outer diameter and beam profiles of the scattering patterns. A series of tests were performed using this apparatus and their results were recorded using a Nikon D7200 digital camera with AF-P Nikkor 18-55 mm lens, manual focus, settings: F11, ISO 125, no flash; and a NEC 38-0620 monochrome beam profiler camera using an 8 mm, F-1.3 zoom lens with manual focus. A Czerny-Turner design spectrometer with Spectrum Studio 1.3 spectrograph software, and beam profiles using Beamview 4.8.1 software, both installed on a Dell Inspiron 14 laptop computer running Windows 7. In a first experiment, a Ferrocell was centrally located inside the Helmholtz inductors, equidistant at 70 mm between laser aperture and target. Laser power output was measured using a SPER Scientific 840011 laser power meter out of the aperture. This reading was 10.5 mW (.0105 J/sec) and was maintained within 1.1 percent throughout all the tests shown here. Measured power output from the Ferrocell was 850  $\mu\text{W}$ , indicating 9.65 mW or a 92 percent absorption in the Ferrofluid thin-film layer without an applied field. Input power to the Helmholtz coil was 600 Watts DC (20 VDC @ 30 A) for a duration of 10 seconds. Coil temperature was 22 C at the beginning of each test. An Alpha Labs GM-2 Gaussmeter was used for field strength measurements that indicated a field that remained homogenous within .91 percent for all tests and in this first test, indicated a field strength of 914 Gauss, using its Hall probe centrally positioned between both inductors at this 70 mm location. A digital camera photo of the first target and a reference laser beam without an induced field is shown in Figure 5a. A beam profile of the laser spot on the second target without an induced field is shown for a reference in Figure 7a. During the ten second period after the coils were activated, a scattered circular pattern was resolved, filling the 55 mm target area and beyond its outer circumference, as shown in Figure 5b. A spectrometer measurement of the beam amplitude, without using a target and expressed in relative units along the y-axis is shown in Figure 6b and a beam profile of the resulting scattering pattern, utilizing the second target, is shown in Figure 7b. We see as the scattering progressed, the laser beam "spot" diminished approximately 60% in amplitude from 6500 (relative linear units) without an EM field, as shown in Figure 6a, then down to 2450 after 10 seconds of the applied electromagnetic field, seen in Figure 6b. In a second experiment, a Ferrocell was positioned closer to the target at a distance of 30 mm within a measured field strength of 885 Gauss. Figure 5c shows a photo of the resulting circular beam scattering pattern on the first target. The outside diameter of the ring measured 30 mm, compared to the previous experiment where the circular ring diameter was larger than the target's 55 mm outer circumference. Figure 6c shows the spectrometer results without an induced field at 5900 while Figure 6d is 2250 with an EM field.

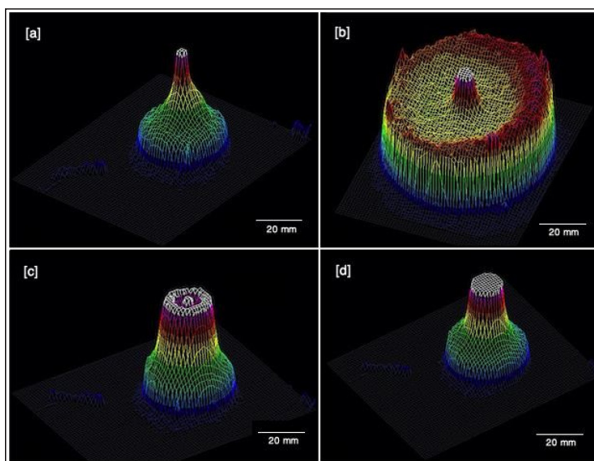


**Figure 5:** Scattering patterns. No EM: [a] 70 mm from target. With EM: [b] 70 mm, [c] 30 mm, [d] 20 mm distance from target.



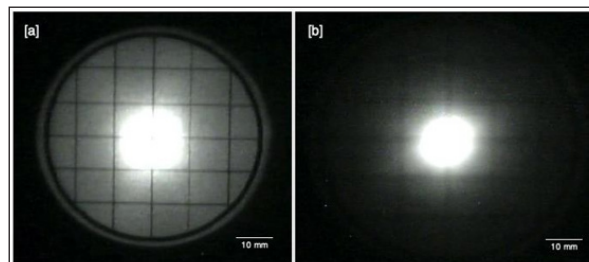
**Figure 6:** Spectrographs of scattering amplitude. [a], No EM @ 70 mm. [b], Absorption at 70 mm. [c], No EM at 30 mm. [d] Absorption at 30 mm. [e], No EM at 20 mm. [f], Absorption at 20 mm.

Figure 7c represents the resultant beam profile at a 30 mm distance from the second target as a 3-D graph. A third experiment was performed using a Ferrocell closer to the north polar end of the field into a measured strength of 837 Gauss. The cell was positioned to a distance of 20 mm from the target. Figure 5d shows a photo of the resulting circular pattern. The outside diameter of this ring was 20 mm, compared to the previous experiment where the ring was 30 mm outside diameter. Figure 6e shows the spectrometer result without an induced field at 6750 while Figure 6f shows the absorption down to 2500 with an EM field. Figure 7d represents the beam profile as a 3-D graph utilizing the second target. The fourth and final experiment for this report was performed for a comparison between the electromagnetic lensing effect obtained from a flat-glass Ferrocell and a typical 35 mm diameter by 6 mm thick Plano-concave lens of VIS coated, frosted, BK-7 glass. A mounting plate for the concave lens was printed using black ABS plastic and it was centrally positioned within the tunnel insert, at an equal distance of 70 mm between aperture and first target.



**Figure 7:** Ferrocell beam profiles. No EM [a] 70 mm. With EM [b] 70 mm, [c] 30 mm, [d] 20 mm from target.

The curved face of the concave lens was irradiated into its center by laser with only 3 mW of output power to obtain a clear, unsaturated photo due to the negligible absorption from the glass. Figure 8a shows this recorded image of the Plano-concave lens's circular beam pattern on the first target with the Ferrocell positioned at 70 mm, and Figure 9a represents the 3-D profile of the glass Plano-concave lens's circular beam dispersion. And in another test with the lens closer to the target, Figure 8b shows a photo from the beam profiling camera of the Plano-concave lens irradiated with 3 mW laser output power at a distance of 35 mm away from the first target. Figure 9b shows a 3-D graphical representation of the Plano-concave lens beam profile at 35 mm distant from the first target. These two tests show typical Gaussian patterns obtained by a glass lens.



**Figure 8:** Beam profiler camera images of Plano-concave lens. [a] at 70 mm and [b] 30 mm from target.

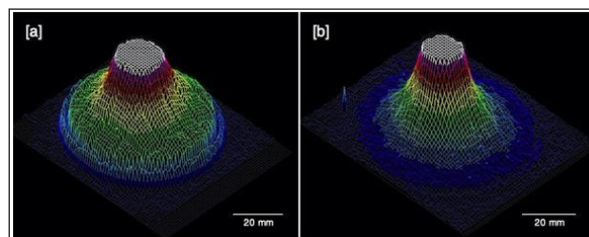


**Figure 9:** Beam profiles of Plano-concave lens. [a] at 70 mm and [b] at 30 mm from target

## Conclusion

I've shown by experiment how a flat-glass Ferrocell will respond when influenced by a parallel electromagnetic field and irradiated with laser and how this field is responsible for diffracting laser through the thin-film into a projected circular beam pattern. These tests indicate a lensing effect from an electromagnetically induced Ferrocell when positioned closer or farther away from the target, thereby altering the circular ring's outer diameter. Also, I've shown a strong correlation to this effect and the lensing effect of laser passing through a glass Plano-concave lens at different distances from the target. It should be noted that the active region of the Ferrocell, when illuminated by the laser is only a one-millimeter circular area and the high currents required to complete these experiments were necessary due to the large surface area of the Ferrocell. This apparatus could be made much smaller and more efficient, but those goals are not within the focus of this investigation. More detailed information about the Ferrocell is available from the referenced papers I've included. The experiments shown in this report can be easily duplicated by anyone with basic technical skills, and I encourage experimental researchers with an interest in this topic to re-create these experiments to verify my findings. Please contact me directly with any questions. I will make the 3-D printer files (stl's) available for the individual pieces of the featured apparatus and instructions on how to construct a Ferrocell, by request.

### Acknowledgments

would like to thank Dr. Alberto Tufaile and his wife, Dr. Adriana Pedrosa Biscaia Tufaile at the School of Arts, Sciences and Humanities in Sao Paulo, Brazil for their continuing support, research and collaboration over the past six years. Additionally, I would like to thank Michael M. Snyder from the University of Louisville, Kentucky, USA, Emmanouil Markoulakis at Hellenic Mediterranean University, Irakleion, Greece, Dr. Rasbindu V. Mehta and Vishakha Dave at Maharaja Krishnakumarsinhji Bhavnagar University, India for their continuing contributions and collaboration utilizing the Ferrocell.

### Disclosures

Funding. Ferrocell USA, LLC. Ligonier, Pennsylvania 15658 USA, A private Research and Development Corporation. The author has a direct interest in this topic, however decided to turn all proprietary information, including his patent, over to public domain in 2018 and continues to investigate the optical properties of a Ferrofluid thin-film in collaboration with other researchers around the world in the interest of science and technology.

TAV: Ferrocell USA

### References

1. Ferrocell® is a registered US Trademark for the magneto-optic device generally known as a Ferrolens. Magnetic flux viewer, US patent 8246356. 2012.
2. Ferrolens is the generic term for the US Trademarked Ferrocell. <https://en.everybodywiki.com/Ferrolens>
3. Alberto Tufaile, Timm A Vanderelli, Adriana Pedrosa Biscaia Tufalie. Light Polarization Using Ferrofluids and Magnetic Fields. *Advances in Condensed Matter Physics*. 2017. 2017: 1-7.
4. Alberto Tufaile, Michael M Snyder, Adriana Pedrosa Biscaia Tufalie. Horocycles of Light in a Ferrocell. 2021. *Condensed Matter*. 6: 30.
5. Alberto Tufaile, Michael M Snyder, Timm A Vanderelli, Adriana Pedrosa Biscaia Tufalie. Jumping Sundogs, Cat's Eye and Ferrofluids. *Condensed Matter*. 2020. 5: 45.
6. Vishakha Dave, Rasbindu V Mehta, SP Bhatnagar. Extinction of light by a Ferrocell and ferrofluid layers: A comparison. *Optik, an International Journal for Light and Electron Optics*. 2020.
7. Emmanouil Markoulakis, Timm Vanderelli, Lambros Frantzeskakis. Real time display with the ferrolens of homogeneous magnetic fields. *Journal of Magnetism and Magnetic Materials*. 2021. 541: 168576.
8. Mehta RV. Polarization dependent extinction coefficients of superparamagnetic colloids in transverse and longitudinal configurations of magnetic field. *Elsevier - Optical Materials*. 2014. 1436-1442.
9. Alexey O Ivanov, Andrey Zubarev. Chain formation and Phase Separation in Ferrofluids: The Influence on Viscous Properties. 2020. 13: 3956.
10. Rosensweig RE. *Ferrohydrodynamics*. Dover publishing 1997. 178-179.
11. Rajesh Regmi, Correy Black, Sudkar C, Keyes PH, Ratna Naik, et al. Department of Physics and Astronomy, Wayne State University, Detroit, MI, USA. Effects of fatty acid surfactants on the magnetic and magnetohydrodynamic properties of ferrofluids. *Journal of Applied Physics*. 2009. 106: 113902.